ChemComm
Chemical Communications

Accepted Manuscript

This article can be cited before page numbers have been issued, to do this please use: L. Li, S. Cui, A. Hu, W. Zhang, Y. Li, N. Zhou, Z. Zhang and X. Zhu, *Chem. Commun.*, 2020, DOI: 10.1039/D0CC01934H.

ROYAL SOCIETY OF CHEMISTRY

rsc.li/chemcomm

View Article Online
DOI: 10.1039/D0CC01934H

COMMUNICATION

Smart Azobenzene-Containing Tubular Polymersomes: Fabrication and Multiple Morphological Tuning

Received 00th January 20xx,
Accepted 00th January 20xx

DOI: 10.1039/x0xx00000x

Lishan Li,[1] Songbo Cui,[3] An Hu,[1] Wei Zhang,[1] Yiwen Li,*[,2] Nianchen Zhou,*[,1] Zhengbiao Zhang [1] and Xiulin Zhu [1]

A fundamental challenge in nano-material science is to elaborately fabricate nonspherical polymersomes. Here, several kinds of novel tubular polymersomes were fabricated via self-assembly of amphiphilic azobenzene-containing block copolymers. Besides, the shape could be tuned by multiple approaches including chemical structure, self-assembly condition and external stimuli.

Morphological control of polymeric nanoparticle via self-assembly is a promising approach to create versatile nano-materials for meeting the needs of development in nano-technological and biomedical fields. Recent developments have demonstrated that the non-spherical nanopaticles assembled from amphiphilic copolymers have made a tremendous impact in a wide range of areas ranging from biomedical to energy area.[1] Among them, the tubular structures have attracted particular interest owing to their unique features such as a large surface area.[2] In nature, the tubular membrane structures are widely existing in eukaryotic cells and some bacteria, which play important roles in several cellular processes.[3] Inspired by this, the tubular polymersomes have also been designed to load with drugs and functional molecules for drug carrier and cellular delivery for biomedical purposes.[2d, 4] Whilst many interesting properties and promising applications of tubular polymersomes have been widely proposed and explored, only limited examples have been reported so far by using osmotic pressure[2e] or chemical addition strategy[5] to transform spherical polymersomes into non-spherical structures.[6] Therefore, it is still highly desirable to seek for new kinds of polymeric amphiphiles and corresponding fabrication strategies towards smart tubular polymersomes with sophisticated stimuli-responsive characters. In recent years, an emerging strategy towards this goal was proposed to use amphiphilic block copolymers containing liquid-crystalline (LC) side chains to fabricate non-spherical polymersomes (LC lattice confinement strategy).[2c, 7] Several kinds of LC moieties such as cholesterol and perylene derivatives have been successfully employed to synthesize the corresponding LC copolymer amphiphiles for further building up the non-spherical polymersome structures.[8] However, limited morphological tuning and stimuli-responsive behaviors of these non-spherical polymersomes were observed and discussed due to limited species of copolymers and inert nature of those LC moieties.

Herein, we strived to address this issue by the construction of a series of smart tubular polymersomes with various morphologies through the solution self-assembly of amphiphilic block copolymers consisting of hydrophilic linear poly (ethylene glycol, PEG) block and hydrophobic brush-like blocks with three types of azobenzene side-chains (PolyAZO). Unlike cholesterol and perylene, azobenzene derivatives were widely established and regarded as a class of photoresponsive LC units, which can undergo reversible trans-cis and cis-trans isomerization upon light irradiation.[9] Note that such photoisomerization was accompanied by the change of molecular size, shape and dipole moment, which could lead to the shape transformation of many azobenzene-containing polymeric nanomaterials such as micelles[10], colloidal spheres[11], vesicle membrane [12] and so on.[13] Moreover, azobenzene was also found to be sensitive to several reductants or enzymes like hydrazine, $Na_2S_2O_4$, or azoreductase, mainly due to the cleavage of the azo bond under reductants conditions.[14] So it was anticipated that the resulting light and reductant dual-responsive tubular polymersomes would expand the library of azobenzene-based nanomaterials.

In this work, we studied the formation of multi-morphological tubular polymersomes from three kinds of amphiphilic azobenzene-containing block copolymers for the first time. We then discussed the shape transformation of these polymersomes by tuning the chemical composition of the azobenzene side-chains (three different types), the fabrication process (i.e. water content in the mixture solvent) and the external stimuli (light and redox).

1. State and Local Joint Engineering Laboratory for Novel Functional Polymeric Materials, Jiangsu Key Laboratory of Advanced Functional Polymer Design and Application, College of Chemistry, Chemical Engineering and Materials Science, Soochow University, Suzhou, 215123, P. R. China.
2. College of Polymer Science and Engineering, State Key Laboratory of Polymer Materials Engineering, Sichuan University, Chengdu, 610065, P. R. China.
3. Department of Chemical Engineering, Waterloo Institute for Nanotechnology, University of Waterloo, 200 University Avenue West, Waterloo N2L 3G1, Ontario, Canada.
*E-mail nczhou@suda.edu.cn. *E-mail: ywli@scu.edu.cn.
Electronic Supplementary Information (ESI) available: Experiments, figures, tables
See DOI: 10.1039/x0xx00000x

The amphiphilic azobenzene-containing block copolymers PEG-b-PolyAZO can be directly prepared by atom transfer radical polymerization (ATRP). Scheme S1 shows synthesis routes and chemical structures of three typical types of PEG-b-PolyAZO, named PEG_{113}-b-$PFAZO_x$, PEG_{113}-b-$PAZO_y$, PEG_{113}-b-$PAZOCN_z$. The AZO composition of PEG-b-PolyAZO could be calculated from ^{1}H NMR spectra (Figure S1), and all PEG-b-PolyAZO samples displayed symmetric peaks with relatively narrow polydispersity indexes (PDI) in GPC elution traces (Figure S2). The detailed macromolecular characterization data of the PEG-b-PolyAZO was summarized in Table S1.

The self-assembly of three types of diblock copolymers PEG-b-PolyAZO was conducted in water/1,4-dioxane. The detailed operation was described in the experiment section. The self-assemblies of PEG_{113}-b-$PFAZO_x$ with different azo-blocks (x=20, 35, 51, 78, 100) (Table S1) were conducted as an example. The morphological transition from micelles (x=20, 35), vesicles (x=51) to tubular polymersomes (x=78, 100) was observed as the length of azo-blocks increased, the details of which were shown in Figure S3. Similar to the PEG_{113}-b-$PFAZO_x$, the other two kinds of amphiphilic copolymers PEG_{113}-b-$PAZO_y$, PEG_{113}-b-$PAZOCN_z$ could also form micelles, vesicles to tubular polymersomes as the hydrophobic fraction increasing under the same self-assembly condition as PEG_{113}-b-$PFAZO_x$. Interestingly, these tubular polymersomes showed different morphologies. For example, the PEG_{113}-b-$PFAZO_{78}$ self-assembled into soft tadpole-like tubular polymersome with one big vesicle of about 470 nm at one end joined by tubular tail with a diameter of 200 nm and a wall thickness of 37 nm (Figure 1a), while the PEG_{113}-b-$PAZO_{64}$ formed the smooth tubular polymersome with a diameter of 200 nm and a wall thickness of 37 nm (Figure 1b), and the PEG_{113}-b-$PAZOCN_{59}$ formed straight and rigid needle-like one with a diameter of 170nm and a wall thickness of 36 nm (Figure 1c). The differences between these tubular polymersomes might be due to the different arrangements of azobenzene units in the tube wall. The lateral ortho-fluorination is known to lower the mesophase thermal stability, the melting point, and the arranging order of the liquid crystal. [15] So, for the PEG_{113}-b-$PFAZO_{78}$, the lower order of the azobenzene molecular means the difficulty of forming long-range order, which induces soft surface topographies of the tadpole-like tubular polymersomes. In addition, the formation of rigid needle-like morphology in PEG_{113}-b-$PAZOCN_{59}$ may be mainly attributed to the liquid-crystalline (LC) arrangements of the 4-cyanoazobenzene LC mesogens during the self-assembly process.[30] The similar morphologies have also been obtained by the self-assembly of block copolymers bearing LC side chains. [6, 7c] The deduction of LC properties of the copolymers PEG-b-PolyAZO and the arrangement of the azobenzene molecules in polymersomes could be confirmed by the DSC and POM data in figure S4. Therefore, we could conclude that a series of tubular polymersomes can be facilely achieved by the self-assembled azobenzene amphiphilic block copolymers and their morphologies can be tuned by changing the chemical composition of azobenzene side chains, as shown in Figure 1.

We then carefully investigated the shape transformation of self-assembled structures of PEG_{113}-b-$PFAZO_{78}$ by tuning the

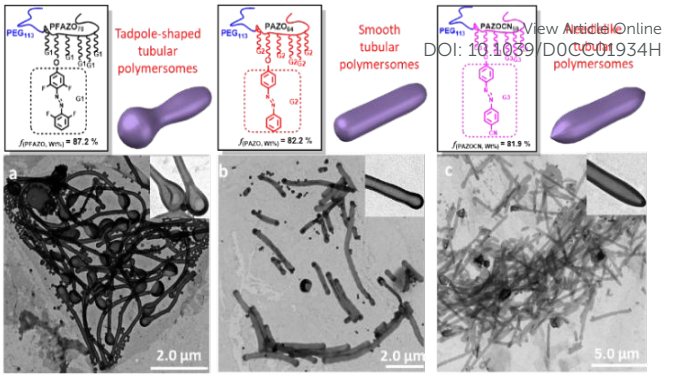

Figure 1. Schematic illustration and TEM images (stained with phosphotungstic acid) of self-assembled morphologies of (a) PEG_{113}-b-$PFAZO_{78}$, (b) PEG_{113}-b-$PAZO_{64}$, (c) PEG_{113}-b-$PAZOCN_{59}$ in water /1,4-dioxane (0.6/1, v /v). The initial concentration was 1.0 mg/mL.

water content in the mixture solvent during the micellar fabrication process. The relevant TEM images were shown in Figure 2a, Figure S5 and Figure S6, and the average size variation was summarized in Table S2. When the water content was 16.6%, large spherical polymersomes with the average particle size of about 1000 nm were mainly observed (Figure S5a). As the water content increasing from 27.1% to 37.5%, the spherical polymersomes began to transfer into tadpole-shaped polymersomes consisting of tapering vesical heads and lengthening tubular tails (Figure S5b; S5c; S6a). The evolution process from vesicles to tubes could be explained by lubensy and prost's theory,[16] which indicated that the development of in-plane orientational order within a vesicle can favour a morphology change from a sphere to a cylinder or a torus when the flexibility of the membrane was low enough. Herein, during the increase of the water content, the dioxane was removed from the hydrophobic layer of vesicle progressively, so that the flexibility of the copolymer membranes could decrease to form the in-plane orientational order. [17]

However, the formation process from huge spherical vesicles to tadpole-shaped tubular polymersomes by budding-like way has rarely been reported so far. We speculated that those transformations might be due to the adsorption process of small nanoparticles by polymersomes, as referring to the tubular process of bacteria[18] and lipid vesicles.[19] From Figure1a, we found that the small vesicles coexisted with the polymersomes, so we suspected that the huge spherical vesicles could catch and fuse the small ones during the self-assembly process. The adsorption and fusion will increase the partial curvature at the syncretic section and further induced the formation of the protrusion. This process was then accompanied, enhanced, by the development of the in-plane orientational order discussed above.[19] If multiple small vesicles adhered to the surfaces of a spherical membrane, multiple protrusions in the polymersomes could also be observed. We can find some tadpole-shaped tubular polymersomes with multi-tails from TEM when the water content was 27.1% (Figure S5d), which offered direct supporting evidence for the adhesion-fusion transformation process discussed above.

When the water content increased to 50.0%, a mixture of tubular polymersomes with single and double-layer membranes formed (Figure S6b). When the water content reached 60%,

almost all tubular polymersomes were turned into bead-like shapes with single-layer (Figure S6c) or double-layer membranes which can be either inherent or caused by collapse/shrinkage of single-layer tubular polymersomes during TEM measurement (Figure S6d). Note that, as shown in Figure S6c, the pipe diameter of the raised part of about 200 nm was similar to the diameter of the smooth tubular tail in Figure S6a, which probably indicated that bead-like tubular polymersome was evolved by partial contraction of the smooth one. The similar phenomenon of vesicle invagination could be found in some literature reported by Kim and van Hest et al., who successfully utilized an osmotic pressure-based strategy to transform spherical polymersomes into stomatocytes and tubular polymersomes. [2e, 20] During the water adding, 1,4-dioxane from the inner compartment of the polymersomes diffused across the bilayer membrane. However, when the water content was large enough, the compact hydrophobic section would hinder the diffusion of the water and accelerate the formation of osmotic pressure difference between the inner and exterior of the polymersomes. Sometimes, the osmotic pressure difference might generate the asymmetric folding of the membrane structures of polymersomes. This phenomenon was popularly found in neuronal axons and blood vessels induced by distinct osmotic stress.[21] After dialysis against ultrapure water, the morphology of these polymersomes remained unchanged even after 4 months (Figure S6e, f). Based on the discussion above, schematic illustration in figure 2b was proposed to discuss the possible morphological transformation from spherical polymersomes to tadpole-shaped tubular polymersomes with the increase of water content in the mixture solvent.

The stimuli-induced morphological variation of these PEG-b-PolyAZO tubular polymersomes by light and reductant was then researched by using the PEG_{113}-b-$PFAZO_{78}$ tubular polymersome as a typical example. As we know, the o-fluoroazobenzene can undergo photoisomerization under green and blue light irradiation.[22] The absorption changes of the PEG_{113}-b-$PFAZO_{78}$ tubular polymersomes under blue/green light irradiation were characterized by UV-vis spectroscopy, as shown in Figure S7. Furthermore, the reversible photoisomerization process could be recycled many times under irradiation with switchable green /blue light (Figure S8).

The morphological transformation of those PEG_{113}-b-$PFAZO_{78}$ tubular polymersomes (water/dioxane=0.6/1 (v/v)) under light irradiation was then investigated by transmittance observation and TEM images. For example, the transmittance of the tubular polymersomes solution was increased to 62% under green light irradiation, while that decreased to 57% under blue light. Such process can be repeated multiple times by alternate irradiation with blue/green light (Figure S9). Figure S10 showed the correlative TEM images in the above process. It was observed that the length of tubular polymersomes decreased to less than 5 microns from 5-10 microns (initiate state) after irradiated with green light (Figure S10a, b), and then returned to 5-10 microns after irradiation with blue light (Figure S10c). The light-triggered change in the diameters of the tubular tails was also observed,

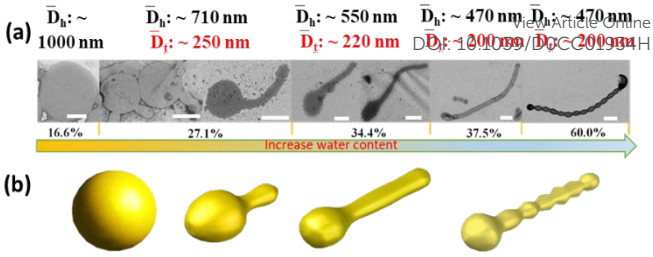

Figure 2. TEM images (a) and corresponding schematic illustration (b) of morphological transformation of PEG_{113}-b-$PFAZO_{78}$ aggregates upon increasing water content from 16.6 %, 27.1%, 34.4% and 37.5% to 60.0% during the micellar preparation process in water /1,4-dioxane. The initial concentration was 1.0 mg/mL. The Dh and Dt represents the head and tail diameter of tadpole-like tubular polymersomes, respectively, and the values come from Table S2. The scale bars are all 500nm in (a).

which were 200 nm, 320 nm and 190 nm at the initial state, cis-state, and trans-state respectively. Simultaneously, the wall thickness was also found to be 37nn, 40nm, 32nm respectively at three different states above (Figure 3a, 3b, 3c). More obvious morphological change from needle-like to smooth tubular polymersomes for PEG_{113}-b-$PAZOCN_{59}$ under light irradiation was observed in Figure S11.[23]

The photoinduced changes of the dipole moment and arrangement mode of azobenzenes in aggregates usually are two main factors for the morphological change of the aggregates during the photoisomerization process.[24] For PEG_{113}-b-$PFAZO_{78}$, the calculated dipole moment of trans/cis isomer is 3.332 D and 7.364 D for the o-fluoroazobenzene derivative (Figure S12). An increase of dipole moment can increase the polarity of the hydrophobic PFAZO block in the tubular polymersomes, which might change the hydrophilic/hydrophobic balance and induce the decrease of the core-corona interfacial energy. Additionally, compared with tightly packed trans-azobenzene, non-planar cis- azobenzene in PFAZO can be fluffy and occupy more volume, which could also weaken intermolecular π-π stacking between the hydrophobic chain, making looser packing mode in hydrophobic layer of the tubular polymersome. [24a] Both the two factors can result in the increase of wall thickness and swelling of tubular polymersome under green light. The possible reason for shape change of PEG_{113}-b-$PAZOCN_{59}$ tubular polymersome was given in Supporting Information.

Moreover, the reductant-responsive properties of tubular polymersomes were investigated selecting hydrazine hydrate as the typical reductant.[14] Shape variation of the PEG_{113}-b-$PFAZO_{78}$ tubular polymersome under hydrazine hydrate at different time was shown in Figure 3d, e, f. For instance, some of the tubular polymersomes were partly dissociated and resulted in lamellar structures after 3 hours reaction (Figure 3e), and further decomposed into many small aggregates after reduction for 20 hours (Figure 3f). Meanwhile, from UV-vis spectroscopy, a remarkable decrease in absorbance around 350 nm was observed after the sample was reduced with hydrazine hydrate for 20h (Figure S13), and the colour change of the solution from yellow to colourless was also observed by the naked eye (inset in Figure S13), indicating that the azo bond was broken. The breakage of the azobenzene moieties weakened hydrophobicity of the core-forming block, resulting in an

View Article Online
DOI: 10.1039/D0CC02541H

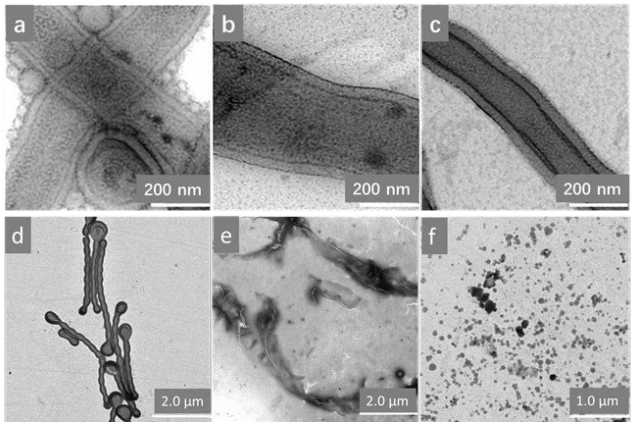

Figure 3. TEM images of the tubular polymersomes of PEG_{113}-b-$PFAZO_{78}$ formed in the water/dioxane (0.6/1.0, v/v; initial concentration: 1.0 mg/mL) before and after light irradiation (a)(b)(c): (a) initial aggregates; (b) aggregates after 532 nm green light irradiation for 5 min (trans-to-cis isomerization); (c) aggregates after 405 nm blue light irradiation for 5 min (cis-to-trans isomerization), treating with hydrazine hydrate for different time (d) (e) (f): (d) initial aggregates; (e) aggregates in the presence of hydrazine hydrate for 3 h; (f) aggregates in the presence of hydrazine hydrate for 20 h.

instability of the tubular polymersomes and subsequent morphological change.

In summary, we have reported the fabrication of multi-morphological tubular polymersomes including tadpole-like, smooth, needle-like and bead-like tubular polymersomes via direct self-assembly of amphiphilic azobenzene-containing block copolymers. We observed that the shape transformation of those tubular polymersomes can be facilely and tuned by changing the chemical structure of azobenzenes or adjusting the water content. In addition, the tubular polymersomes showed light and redox dual-responsive behaviours, which could also induce the shape transformation. These novel smart tubular polymersomes show promising potential applications in stimuli-responsive nanomaterials such as specific switching devices and polymeric nano-vehicles for loading cargo with triggering release. More research on these tubular polymersomes will be of great necessity.

This work was supported by the National Science Foundation of China (21871202, 21925107), the Priority Academic Program Development of Jiangsu Higher Education Institutions (PAPD), the Program of Innovative Research Team of Soochow University and Collaborative Innovation Center of Suzhou Nano Science and Technology.

Conflicts of interest

There are no conflicts to declare.

Notes and references

1. (a) O. Mhatre and S. Sodha, *Nanomedicine*, 2019, **18**, 243-258; (b) B. Yu, H. Cong, Q. Peng, C. Gu, Q. Tang, X. Xu, C. Tian and F. Zhai, *Adv Colloid Interface Sci*, 2018, **256**, 126-151; (c) Xu, H. Qian and S. Lin, *ACS Macro Letters*, 2020, **9**, 404-409; (d) C. Feng and X. Huang, *Acc Chem Res*, 2018, **51**, 2314-2323; (e) D. Tao, C. Feng, Y. Cui, X. Yang, I. Manners, M. A. Winnik and X. Huang, *J. Am. Chem. Soc.*, 2017, **139**, 7136-7139; (f) D. Tao, C. Feng, X. Yang, I. Manners, M. A. Winnik and X. Huang, *Macromolecules*, 2018, **51**, 2065-2075;
2. (a) X. L. Sun, D. M. Liu, S. Pei, K. K. Li and W. M. Wan, *ACS Macro Lett.*, 2016, **5**, 1180-1184; (b) X. L. Sun, D. M. Liu, P. Wang, J. L. Tan, K. K. Li, L. Deng and W. M. Wan, *Chem. Commun.*, 2017, **53**, 5005-5008; (c) L. Jia, P. A. Albouy, A. Di Cicco, A. Cao and M. H. Li, *Polymer*, 2011, **52**, 2565-2575; (d) J. D. Robertson, G. Yealland, M. Avila-Olias, L. Chierico, O. Bandmann, S. A. Renshaw and G. Battaglia, *ACS Nano*, 2014, **8**, 4650-4661; (e) L. K. E. A. Abdelmohsen, D. S. Williams, R. S. M. Rikken, D. A. Wilson and J. C. M. van Hest, *J. Am. Chem. Soc.*, 2016, **138**, 9353-9356.
3. G. K. P. Voeltz, W. A., *Nat. Rev. Mol. Cell Biol.*, 2007, **8**, 258-264.
4. B. M. Blunden , R. Chapman, M. Danial, H. Lu, K. A. Jolliffe, S. Perrier and M. H. Stenzel, *Chem. Eur. J.*, 2014, **20**, 12745-12749.
5. M. C. M. van Oers, F. P. J. T. Rutjes and J. C. M. van Hest, *J. Am. Chem. Soc.*, 2013, **135**, 16308-16311.
6. C. K. Wong, M. H. Stenzel and P. Thordarson, *Chem. Soc. Rev.*, 2019, **48**, 4019-4035.
7. (a) L. Jia, A. Cao, D. Lévy, B. Xu, P. A. Albouy, X. Xing, M. J. Bowick and M. H. Li, *Soft Matter*, 2009, **5**, 3446-3451; (b) X. Xing, H. Shin, M. J. Bowick, Z. Yao, L. Jia and M. H. Li, *Proc. Natl. Acad. Sci. India Sect. B (Biol. Sci.)*, 2012, **109**, 5202-5206; (c) L. Jia, D. Lévy, D. Durand, M. Impéror-Clerc, A. Cao and M. H. Li, *Soft Matter*, 2011, **7**, 7395-7403.
8. C. K. Wong, A. F. Mason, M. H. Stenzel and P. Thordarson, *Nat. Commun.*, 2017, **8**, 1240.
9. C. W. Chang, Y. C. Lu, T. T. Wang and E. W. G. Diau, *J. Am. Chem. Soc.*, 2004, **126**, 10109-10118.
10. (a) G. Wang, X. Tong and Y. Zhao, *Macromolecules*, 2004, **37**, 8911-8917; (b) J. Wu, B. Xu, Z. Liu, Y. Yao, Q. Zhuang and S. Lin, *Polym. Chem.*, 2019, **10**, 4025-4030.
11. Y. Li, Y. He, X. Tong and X. Wang, *J. Am. Chem. Soc.*, 2005, **127**, 2402-2403.
12. J. del Barrio, L. Oriol, C. Sánchez, J. L. Serrano, A. Di Cicco, P. Keller and M. H. Li, *J. Am. Chem. Soc.*, 2010, **132**, 3762-3769.
13. (a) T. Seki, H. Sekizawa, S.-y. Morino and K. Ichimura, *J. Phys. Chem. B*, 1998, **102**, 5313-5321; (b) W. Wang, D. Shen, S. W. Hong and Z. Lin, *angew. chem. int. ed.*, 2018, **57**, 2139-2143.
14. (a) W. X. Gu, Q. L. Li, H. Lu, L. Fang, Q. Chen, Y. W. Yang and H. Gao, *Chem. Commun.*, 2015, **51**, 4715-4718; (b) J. Wang, S. Li, B. Wu and Y. He, *Eur. Polym. J.*, 2016, **84**, 236-244; (c) D. Zhou, Y. Wang, J. Jia, W. Yu, B. Qu, X. Li and X. Sun, *Chem. Commun.*, 2015, **51**, 10656-10659; (d) J. Rao and A. Khan, *J. Am. Chem. Soc.*, 2013, **135**, 14056-14059.
15. (a) G. W. Gray, M. Hird, D. Lacey and K. Toyne, *J. Chem. Soc. Perk. 2T. 2*, 1989, 2041-2053; (b) A. Matharu and D. Chambers-Asman, *Liq. Cryst.*, 2007, **34**, 1317-1336; (c) G. Gray, M. Hird, D. Lacey and K. Toyne, *Mol. Cryst. Liquid Cryst.*, 1989, **172**, 165-189.
16. T. Lubensky and J. Prost, *Journal de Physique II*, 1992, **2**, 371-382.
17. K. Yu and A. Eisenberg, *Macromolecules*, 1998, **31**, 3509-3518.
18. M. Leaver, P. Dominguez-Cuevas, J. Coxhead, R. Daniel and Errington, *Nat. Commun.*, 2009, **457**, 849.
19. Y. Yu and S. Granick, *J. Am. Chem. Soc.*, 2009, **131**, 14158-14159.
20. K. T. Kim, J. Zhu, S. A. Meeuwissen, J. J. Cornelissen, D. J. Pochan, R. J. Nolte and J. C. van Hest, *J. Am. Chem. Soc.*, 2010, **132**, 12522-12524.
21. P. A. Pullarkat, P. Dommersnes, P. Fernandez, J. F. Joanny and A. Ott, *Phys. Rev. Lett.*, 2006, **96**, 048104.
22. D. Bléger, J. Schwarz, A. M. Brouwer and S. Hecht, *J. Am. Chem. Soc.*, 2012, **134**, 20597-20600.
23. (a) D. Wang, H. Ren, X. Wang and X. Wang, *Macromolecules*, 2008, **41**, 9382-9388; (b) M. Han, K. Ichimura, P. Ramanujam and S. Hvilsted, *Macromolecules*, 2001, **34**, 4256-4262.
24. (a) X. Tong, G. Wang, A. Soldera and Y. Zhao, *J. Phys. Chem. B*, 2005, **109**, 20281-20287; (b) Q. Ye, M. Huo, M. Zeng, L. Liu, L. Peng, X. Wang and J. Yuan, *Macromolecules*, 2018, **51**, 3308-3314; (c) S. Guan, C. Zhang, W. Wen, T. Qu, X. Zheng, Y. Zhao and A. Chen, *ACS Macro Lett.*, 2018, **7**, 358-363.